Fourier diffraction theorem for diffusion-based thermal tomography

2006 J. Phys. A: Math. Gen. 39 14379

(http://iopscience.iop.org/0305-4470/39/46/010)

INSTITUTE OF PHYSICS PUBLISHING JOURNAL OF PHYSICS A: MATHEMATICAL AND GENERAL

J. Phys. A: Math. Gen. **39** (2006) 14379–14395 doi:10.1088/0305-4470/39/46/010

Fourier diffraction theorem for diffusion-based thermal tomography

Natalie Baddour

Department of Mechanical Engineering, University of Ottawa, 161 Louis Pasteur, Ottawa, K1N 6N5, Canada

E-mail: nbaddour@eng.uottawa.ca

Received 31 July 2006, in final form 5 October 2006
Published 1 November 2006
Online at stacks.iop.org/JPhysA/39/14379

Abstract

There has been much recent interest in thermal imaging as a method of non-destructive testing and for non-invasive medical imaging. The basic idea of applying heat or cold to an area and observing the resulting temperature change with an infrared camera has led to the development of rapid and relatively inexpensive inspection systems. However, the main drawback to date has been that such an approach provides mainly qualitative results. In order to advance the quantitative results that are possible via thermal imaging, there is interest in applying techniques and algorithms from conventional tomography. Many tomography algorithms are based on the Fourier diffraction theorem, which is inapplicable to thermal imaging without suitable modification to account for the attenuative nature of thermal waves. In this paper, the Fourier diffraction theorem for thermal tomography is derived and discussed. The intent is for this thermal-diffusion based Fourier diffraction theorem to form the basis of tomographic reconstruction algorithms for quantitative thermal imaging.

PACS numbers: 02.30.Zz, 02.60.Nm, 05.70.−a, 44.00.00
Mathematics Subject Classification: 80A20, 80A17, 80A23, 45Q05

(Some figures in this article are in colour only in the electronic version)

1. Introduction

Due to the increasing availability of low-cost high-performance infrared cameras, thermal imaging has become one of the fastest growing areas of non-destructive testing. These newer cameras have promoted the development of thermal inspection systems with improved detection capability and spatial resolution. The basic premise is to apply heat to a material and to subsequently observe the way the surface temperature evolves in order to glean information about the internal composition and state of the material. The technique can

be rapid, relatively inexpensive and, more importantly, has the capability to cover a large area in a single inspection measurement (Avdelidis *et al* 2004, Quek and Almond 2005, Quek *et al* 2005). However, the main shortcoming to date is that thermal imaging is primarily a qualitative technique. At this point in time, thermal imaging provides good qualitative information about the material being inspected and less quantitative information about the size, shape and precise location (specifically, depth) of potential flaws. Additionally, thermal imaging provides less information about the nature or composition of a material than competing techniques such as ultrasound. Along with industrial application, thermal wave imaging has also begun to be applied for medical applications and imaging of biological materials (Telenkov *et al* 2002).

One of the main research goals in thermal imaging is improved flaw/object definition through image processing. There have been some attempts to implement tomographic principles for thermal imaging, with some success (Nicolaides and Mandelis 1997, Nicolaides *et al* 1997, Pade and Mandelis 1994). One difficulty with thermal diffusion imaging is that conventional tomography algorithms are based on the wave equation and thus rely on wave propagation (be it electromagnetic or acoustic). These algorithms are thus inapplicable to thermal diffusion phenomena without appropriate modification.

Similar to sound and electromagnetism, conductive heat propagation is governed by a well-established partial differential equation involving fundamental material parameters such as heat capacity, thermal conductivity, diffusivity and density. Hence, in principle thermal studies should be capable of yielding quantitative material characterization information in a similar manner as its wave-equation-based cousins. Since thermal techniques have shown themselves capable of generating subsurface information inexpensively and quickly, there is motivation behind developing the appropriate mathematics to yield quantitative material information. Tomographic imaging is a possible avenue for extracting quantitative information from thermal measurements.

One approach to thermal tomography has been based on the use of the pseudowave propagation analogy. If a harmonically varying thermal source is introduced, the governing diffusion partial differential equation for heat conduction becomes the Helmholtz pseudowave equation (Mandelis 2001). The resulting solution is a pseudowave that is highly dispersive and attenuative. The wave number governing the propagation of this pseudowave is now complex instead of purely real as with the regular wave equation. It is the complex nature of the wave number that completely changes the nature of the wave propagation and renders the conventional tomographic algorithms inapplicable without suitable modification and interpretation. Mandelis *et al* have considered this diffusion-based approach to thermal tomography (Nicolaides and Mandelis 1997, Nicolaides *et al* 1997, Pade and Mandelis 1994), where this problem was approached from the point of view of discretizing and inverting Green's function. Green's function was discretized in the spatial domain, without resort to transformation into a frequency domain. The researchers correctly noted that the problem is ill-posed and some form of regularization is required. In another approach the use of the spatial Laplace transform was considered as the potential basis for tomographic algorithms (Mandelis 1991); however, this approach necessitates the inversion of a Laplace transform, a non-trivial task. To the best of this author's knowledge, no tomographic algorithms have been developed based on the Laplace transform.

The consideration of a Fourier frequency domain approach to thermographic imaging does not appear to have been previously considered. On the other hand, much of the success of the conventional tomography is based on the Fourier diffraction theorem (Slaney and Kak 1988). Hence, a Fourier domain approach to thermographic imaging would appear to be worthy of further investigation. As previously mentioned, due the diffusive nature of thermal phenomena, the standard Fourier diffraction theorem is inapplicable to thermal tomography

without suitable adaptation. It is this adaptation that is sought in this paper. The main goal of this work is to show how the Fourier diffraction theorem can be adapted to accommodate the diffusion phenomena and thus the complex nature of the wave vector. We approach the solution of the forward problem using the diffusion Helmholtz equation from the point of view of (Fourier) diffraction tomography. Detection in a plane is assumed but our problem formulation does not require plane wave illumination. The forward problem formulation is then specialized to the case of plane wave illumination in order to derive the thermal version of the Fourier diffraction theorem. We discuss the region of the three-dimensional (3D) Fourier transform of the object that is obtained in the detection plane. In this development, the assumptions regarding geometry and the size of the object are kept similar to those used in standard diffraction tomography in order to be able to compare the results of the thermal version of the Fourier diffraction theorem with the well-known results of the standard version.

2. Background theory

The temperature field in a solid is governed by the thermal diffusion equation and is given by

$$\nabla \cdot (K(\vec{r})\nabla T(\vec{r},t)) - \rho(\vec{r})c(\vec{r})\frac{\partial T(\vec{r},t)}{\partial t} = -q(\vec{r},t) \quad \text{in } D \tag{1}$$

where D is the interior of the domain, $(\vec{r})$ is the position vector, t is time, T is the temperature, $q = q(\vec{r},t)$ is the energy generated per unit volume, $K = K(\vec{r})$ is the thermal conductivity, $\rho(\vec{r})$ is the density of the material and $c(\vec{r})$ is the specific heat. Recall that

$$\alpha(\vec{r}) = \frac{K(\vec{r})}{\rho(\vec{r})c(\vec{r})} \tag{2}$$

is the local thermal diffusivity of the material.

This form of the heat equation is more complicated than required. We proceed as in the case of standard diffraction tomography by considering only one temporal frequency at a time. This decomposition is accomplished by finding the Fourier transform of the field with respect to time at each position $\vec{r}$. Noting that the differential equation is linear, the solutions for different frequencies can be added to find additional solutions. If we additionally assume that the thermal conductivity does not vary greatly in space, then taking the Fourier transform leads to the Helmholtz equation

$$(\nabla^2 + k^2(\vec{r}))T(\vec{r},\omega) = -\frac{q(\vec{r},\omega)}{K(\vec{r})} \tag{3}$$

where

$$k^2(\vec{r}) = -\frac{\mathrm{i}\omega}{\alpha(\vec{r})} \tag{4}$$

is the complex wave number. A couple of notes are in order about the preceding statements. First, we define the Fourier transform in the conventional way as

$$\hat{F}(\omega) = \int_{-\infty}^{\infty} f(t)\,\mathrm{e}^{-\mathrm{i}\omega t}\,\mathrm{d}t. \tag{5}$$

With the inverse transform defined by

$$f(t) = \frac{1}{2\pi}\int_{-\infty}^{\infty} \hat{F}(\omega)\,\mathrm{e}^{\mathrm{i}\omega t}\,\mathrm{d}\omega. \tag{6}$$

Secondly, the explicit dependence of T and q on the frequency ω is usually neglected but is still nevertheless implied. Finally, we note that if harmonic excitation is assumed, this leads

to the same Helmholtz pseudowave equation as long as the harmonic excitation is assumed to have the form $I(\vec{r},t) = I_0(\vec{r})\,\mathrm{e}^{\mathrm{i}\omega t}$. If the often-used form of $I(\vec{r},t) = I_0(\vec{r})\,\mathrm{e}^{-\mathrm{i}\omega t}$ (note the change in sign in the exponent) is assumed instead, then the complex wave number is changed by a minus sign, changing the phase of any resulting calculations. This point has no analogue in the wave equation as the presence of the double time derivative in the wave equation leads to the same equation regardless of the sign in the exponent of the assumed harmonic excitation. Harmonic sources are often used for the generation of thermal waves in solids (Mandelis 2001). However, the use of a Fourier transform approach does not limit the time dependence of the source to be harmonic and allows for greater freedom in the analysis of possible sources that can be used.

For imaging purposes, our main interest lies in inhomogeneous media. We therefore consider the Helmholtz equation

$$(\nabla^2 + k^2(\vec{r}))T(\vec{r}) = 0. \tag{7}$$

We now write

$$k^2(\vec{r}) = k_0^2 n^2(\vec{r}) \qquad \text{and} \qquad n^2(\vec{r}) = \frac{\alpha_0}{\alpha(\vec{r})} \tag{8}$$

where $k_0^2 = -\frac{\mathrm{i}\omega}{\alpha_0}$ and α_0 is the thermal diffusivity of the assumed homogeneous medium surrounding the object region Q. Additionally, $n(\vec{r})$ is a measure of the variation of the values of the thermal diffusivity in the scattering object from that of the surrounding homogeneous (reference) region. In general, it is assumed that the object has finite size. This leads to

$$\left(\nabla^2 + k_0^2\right)T(\vec{r}) = -o(\vec{r})T(\vec{r}) \tag{9}$$

where the object function is given by

$$o(\vec{r}) = \begin{cases} k_0^2(n^2(\vec{r}) - 1) & \vec{r} \in Q \\ 0 & \vec{r} \notin Q. \end{cases} \tag{10}$$

We note that the preceding follows exactly the development of the diffraction tomography problem with the wave equation, with the exception of the complex nature of the wave vector. The effect of the inhomogeneities of the object region appears as a source term on the right-hand side of the Helmholtz equation (9), with $o(\vec{r})$ being the object function and representing the inhomogeneities of the scattering object region Q. The object function is zero outside the object region and its non-zero value represents the ratio of thermal diffusivities inside the object region.

We will consider the temperature field $T(\vec{r})$ to be the sum of two components, $T_0(\vec{r})$ and $T_s(\vec{r})$, that is

$$T(\vec{r}) = T_0(\vec{r}) + T_s(\vec{r}). \tag{11}$$

The component $T_0(\vec{r})$ is known as the incident field (or equivalently the illumination function) and is the field present without any inhomogeneities. It is thus given by the solution to

$$\left(\nabla^2 + k_0^2(\vec{r})\right)T_0(\vec{r}) = 0. \tag{12}$$

The component $T_s(\vec{r})$, known as the scattered field, will be that part of the total field that can be attributed solely to the inhomogeneities. The scattered component of the field will necessarily have to satisfy

$$\left(\nabla^2 + k_0^2\right)T_s(\vec{r}) = -o(\vec{r})T(\vec{r}). \tag{13}$$

This scalar Helmholtz equation cannot be solved for $T_s(\vec{r})$ directly, but a solution can be written in terms of Green's function:

$$T_s(\vec{r}) = \int g(\vec{r}|\vec{r}_0)o(\vec{r}_0)T(\vec{r}_0)\,\mathrm{d}\vec{r}_0. \tag{14}$$

Note that the T under the integral sign is the unknown total thermal-wave field and that the integration must be taken over the domain of interest. Green's function is a solution of the differential equation

$$\left(\nabla^2 + k_0^2\right) g(\vec{r}|\vec{r}_0) = -\delta(\vec{r} - \vec{r}_0) \tag{15}$$

and is normally only a function of the difference $\vec{r} - \vec{r}_0$. An approximate solution for $T_s(\vec{r})$ can be written using the Born approximation, which is valid for objects that are weakly inhomogeneous (Slaney and Kak 1988) where the scattering field is weak and much smaller than the total field. The consequence of the Born approximation is that the unknown total field under the integral sign can be replaced with the known incident field. Along with the dependence of Green's function on the difference of position only, this leads to

$$T_s(\vec{r}) = \int g(\vec{r} - \vec{r}_0) o(\vec{r}_0) T_0(\vec{r}_0)\, \mathrm{d}\vec{r}_0. \tag{16}$$

The actual expressions for Green's function and incident field will depend on the choice of geometry and background medium. We note again that the development above follows that of the standard diffraction tomography approach for wavefields that satisfy the wave equation as both approaches lead to the Helmholtz equation. Where the approach for thermal wave fields differs is in the nature of the wave vector k which is purely real for waves satisfying the wave equation but is a complex quantity for thermal wave fields satisfying the heat equation.

Thus far the development has been fairly general and is applicable to various geometries. As for standard diffraction tomography theory, we now assume a background medium infinite in extent and an inhomogeneity structure of finite extent. The above equation for the scattered field is the most general form of the forward problem, valid for all points outside the inhomogeneity and for arbitrary source–detector configurations. Although the assumption of an infinite domain may not be the most physically realistic assumption, it is the simplest case for physical insight and can later be modified for different geometries. As it is also the assumption made for standard diffraction tomography, this assumption will allow for straightforward comparisons.

We further specialize our formulation to the case where the scattered thermal-wave is measured by a plane of detectors. We are interested in the Fourier transform of the wave measured in the $z = z_d$ plane. Since we are interested in detection in one of the z planes, we will first consider the Weyl expansion for the 3D infinite space Green's function.

3. Weyl expansion of 3D infinite space Green's function

Consider a three-dimensional infinite domain. The thermal wave Green's function satisfies

$$\left(\nabla^2 + k_0^2\right) g(\vec{r}|\vec{r}_0) = -\delta(\vec{r} - \vec{r}_0) \tag{17}$$

where $k_0^2 = -\frac{\mathrm{i}\omega}{\alpha_0}$. The three-dimensional infinite domain Green's function is given by (Mandelis 2001, Slaney and Kak 1988)

$$g(\vec{r}|\vec{r}_0) = \frac{\mathrm{e}^{\mathrm{i}k_0|\vec{r}-\vec{r}_0|}}{4\pi|\vec{r} - \vec{r}_0|} = g(\vec{r} - \vec{r}_0). \tag{18}$$

By taking the Fourier transform of the partial differential equation (17) with the impulsive source at $\vec{r}_0 = \mathbf{0}$, we can formally write the three-dimensional Fourier transform of Green's function as

$$\hat{G}(\omega_x, \omega_y, \omega_z) = \frac{1}{\omega_x^2 + \omega_y^2 + \omega_z^2 - k_0^2} = \frac{1}{\omega_z^2 + \gamma_\omega^2}, \tag{19}$$

where $\gamma_\omega^2 = \omega_x^2 + \omega_y^2 - k_0^2$ and $(\omega_x, \omega_y, \omega_z)$ are the spatial frequency variables in the Fourier domain. We can now write Green's function as the inverse Fourier transform of its Fourier transform:

$$\begin{aligned} g(\vec{r}) &= \frac{1}{(2\pi)^3} \int_{-\infty}^{\infty}\int_{-\infty}^{\infty}\int_{-\infty}^{\infty} \frac{1}{\omega_z^2 + \gamma_\omega^2} \, \mathrm{e}^{\mathrm{i}\omega_x x} \, \mathrm{e}^{\mathrm{i}\omega_y y} \, \mathrm{e}^{\mathrm{i}\omega_z z} \, \mathrm{d}\omega_x \, \mathrm{d}\omega_y \, \mathrm{d}\omega_z \\ &= \frac{1}{(2\pi)^2} \int_{-\infty}^{\infty}\int_{-\infty}^{\infty} \mathrm{e}^{\mathrm{i}\omega_x x} \, \mathrm{e}^{\mathrm{i}\omega_y y} \, \mathrm{d}\omega_x \, \mathrm{d}\omega_y \frac{1}{2\pi} \int_{-\infty}^{\infty} \frac{1}{\omega_z^2 + \gamma_\omega^2} \, \mathrm{e}^{\mathrm{i}\omega_z z} \, \mathrm{d}\omega_z. \end{aligned} \tag{20}$$

The integral over spatial frequency ω_z can be done by using residue theory. There are two poles in the integral over ω_z, namely $\omega_z = \pm \mathrm{i}\gamma_\omega = \pm \mathrm{i}(\gamma_{\omega r} + \mathrm{i}\gamma_{\omega i})$, where $\gamma_{\omega r}$ denotes the real part of γ_ω and $\gamma_{\omega i}$ denotes the imaginary part. We define $\gamma_{\omega r}$ and $\gamma_{\omega i}$ such that $\gamma_{\omega r} > 0$. For $z > 0$, we require the imaginary part of ω_z (which is $\gamma_{\omega r}$) to be >0 in order to ensure convergence of the integral over ω_z; therefore $\omega_z = +\mathrm{i}\gamma_\omega$. Therefore, we choose the pole in the upper half plane and a contour integral in the counterclockwise direction in the upper half plane:

$$\frac{1}{2\pi} \int_{-\infty}^{\infty} \frac{1}{\omega_z^2 + \gamma_\omega^2} \, \mathrm{e}^{\mathrm{i}\omega_z z} \, \mathrm{d}\omega_z = \frac{1}{2\pi} 2\pi \mathrm{i} \frac{\mathrm{e}^{-\gamma_\omega z}}{2\mathrm{i}\gamma_\omega} = \frac{\mathrm{e}^{-\gamma_\omega z}}{2\gamma_\omega} \qquad z > 0. \tag{21}$$

Similarly, for $z < 0$ we require the imaginary part of $\omega_z < 0$ for convergence so that $\omega_z = -\mathrm{i}\gamma_\omega$. Therefore we choose the pole in the lower half plane and a *clockwise* contour integral in the lower half plane. The clockwise integral will introduce an extra minus sign when using the residue theory. Therefore, for $z < 0$ we have

$$\frac{1}{2\pi} \int_{-\infty}^{\infty} \frac{1}{\omega_z^2 + \gamma_\omega^2} \, \mathrm{e}^{\mathrm{i}\omega_z z} \, \mathrm{d}\omega_z = \frac{1}{2\pi} (-2\pi \mathrm{i}) \frac{\mathrm{e}^{\gamma_\omega z}}{-2\mathrm{i}\gamma_\omega} = \frac{\mathrm{e}^{\gamma_\omega z}}{2\gamma_\omega} \qquad z < 0. \tag{22}$$

Combining the two expressions for $z > 0$ and $z < 0$, we can write the inner integral more compactly as

$$\frac{1}{2\pi} \int_{-\infty}^{\infty} \frac{1}{\omega_z^2 + \gamma_\omega^2} \, \mathrm{e}^{\mathrm{i}\omega_z z} \, \mathrm{d}\omega_z = \frac{\mathrm{e}^{-\gamma_\omega |z|}}{2\gamma_\omega}. \tag{23}$$

Therefore Green's function in an infinite three-dimensional domain can be written as

$$g(\vec{r}) = \frac{1}{(2\pi)^2} \int_{-\infty}^{\infty}\int_{-\infty}^{\infty} \frac{\mathrm{e}^{-\gamma_\omega |z|}}{2\gamma_\omega} \, \mathrm{e}^{\mathrm{i}\omega_x x} \, \mathrm{e}^{\mathrm{i}\omega_y y} \, \mathrm{d}\omega_x \, \mathrm{d}\omega_y. \tag{24}$$

Note that it is important for convergence reasons to define γ_ω as the square root of $\gamma_\omega^2 = \omega_x^2 + \omega_y^2 - k_0^2$ such that the real part of γ_ω is positive. We clearly recognize the inverse Fourier transform in the ω_x and ω_y variables in the above expression. Therefore, taking the forward Fourier transform of Green's function with respect to x and y *only* (so that $x \to \omega_x$ and $y \to \omega_y$) yields the Weyl expansion for Green's function as

$$g(\omega_x, \omega_y, z) = \frac{\mathrm{e}^{-\gamma_\omega |z|}}{2\gamma_\omega}. \tag{25}$$

The Weyl expansion is effectively a Fourier transform of Green's function (18) with respect to the x and y variables only so that we are looking at Green's function in frequency space for x and y but real space for z. The utility of this expression becomes apparent when using a detection scheme such that the signal is detected on a plane for which z is a constant.

3.1. Alternative derivation of Weyl expansion

The above development suggests a simpler derivation to the Weyl expansion. We start once again with the definition of Green's function with an impulse source at 0:

$$\left(\nabla^2 + k_0^2\right) g(\vec{r}) = -\delta(\vec{r}) = -\delta(x)\delta(y)\delta(z). \tag{26}$$

We take the Fourier transform of both sides of the above equation; however, this time only with respect to the x and y variables leaving the z variable untransformed. This gives

$$\begin{aligned} &\left(\frac{\mathrm{d}^2}{\mathrm{d}z^2} + \left(k_0^2 - \omega_x^2 - \omega_y^2\right)\right) g(\omega_x, \omega_y; z) = -\delta(z) \\ &\left(\frac{\mathrm{d}^2}{\mathrm{d}z^2} - \gamma_\omega^2\right) g(\omega_x, \omega_y; z) = \left(\frac{\mathrm{d}^2}{\mathrm{d}z^2} + (\mathrm{i}\gamma_\omega)^2\right) g(\omega_x, \omega_y; z) = -\delta(z). \end{aligned} \tag{27}$$

We now observe that this is simply the equation for a one-dimensional Green's function in an infinite domain and we can immediately write (Mandelis 2001)

$$g(\omega_x, \omega_y, z) = \frac{\mathrm{e}^{-\gamma_\omega |z|}}{2\gamma_\omega}. \tag{28}$$

This is the same expression we previously obtained through a more laborious derivation. Once again, the definition of γ_ω as the square root of $\gamma_\omega^2 = \omega_x^2 + \omega_y^2 - k_0^2$ such that the real part of γ_ω is positive is crucial in order to keep Green's function well behaved at infinity. Furthermore, we note that a consequence of the real part of γ_ω being positive is that the amplitude decays exponentially as a function of distance z away from the point source. Plane waves with large spatial frequencies will thus have negligible amplitudes. This is a characteristic difference between thermal waves and ordinary ultrasound waves. The thermal plane waves will be scattered by the inhomogeneities and their resulting amplitudes and phases will carry information about the structure of the inhomogeneity.

4. Fourier diffraction theorem

Armed with the Weyl expansion for the 3D infinite space Green's function, we now proceed to derive the thermal Fourier diffraction theorem. We start once again with the first Born approximation, expressed in terms of the differential equation formulation of the problem:

$$\left(\nabla^2 + k_0^2\right) T_s(\vec{r}) = -o(\vec{r}) T_0(\vec{r}). \tag{29}$$

Recall that the first Born approximation is only valid when the scattered field is much smaller than the incident field. We now take the Fourier transform of the governing equation where the Fourier transform is taken in terms of the x and y variables only. The z variable is not transformed since we have restricted our interest to detecting the scattered wave in a $z =$ constant plane. Fourier transformation leads to

$$\begin{aligned} &\left(\frac{\mathrm{d}^2}{\mathrm{d}z^2} + \left(k_0^2 - \omega_x^2 - \omega_y^2\right)\right) T_s(\omega_x, \omega_y; z) = -O(\omega_x, \omega_y; z) T_0(\omega_x, \omega_y; z) \\ &\left(\frac{\mathrm{d}^2}{\mathrm{d}z^2} + (\mathrm{i}\gamma_\omega)^2\right) T_s(\omega_x, \omega_y; z) = -O(\omega_x, \omega_y; z) T_0(\omega_x, \omega_y; z). \end{aligned} \tag{30}$$

The above equation is a simple ODE in the variable z with ω_x, ω_y as parameters. Green's function is exactly that given by the Weyl expansion as derived above. Therefore, the solution to this equation can be immediately written as

$$T_s(\omega_x, \omega_y; z) = \int_{-\infty}^{\infty} O(\omega_x, \omega_y; z') T_0(\omega_x, \omega_y; z') \frac{\mathrm{e}^{-\gamma_\omega |z - z'|}}{2\gamma_\omega} \mathrm{d}z'. \tag{31}$$

This equation tells us that the scattered thermal wave is a convolution of the Weyl function (which is really an expression of Green's function) with the product of the object and illumination functions. Let us refer to this product of the object function with the illumination function as the heterogeneity function. The above equation implies that at any given spatial frequency ω_x, ω_y, the heterogeneity function can be thought of as the source terms for the scattered waves. The plane waves arising from different depths z' propagate along the z direction to the detection plane. During propagation, these waves experience different amplitude and phase variations which are given by $\frac{\mathrm{e}^{-\gamma_\omega |z_d - z_j|}}{2\gamma_\omega}$ for a source located at $z = z_j$ and detected at $z = z_d$. The scattered thermal wave detected at the plane $z = z_d$ is thus a sum (integral) of the plane waves originating from the heterogeneity functions at different depths. The propagation of the heterogeneity function at different depths is weighted by the amplitude attenuation and phase shift given by the Weyl expansion of Green's function. The amplitude and phase of the Weyl expansion depend on the spatial frequencies ω_x, ω_y as well as the distance between the detection plane and the source term. As the spatial frequencies ω_x, ω_y increase, the amplitude of the Weyl expansion decays more quickly and thus Green's function effectively acts as a low pass filter for spatial frequencies.

The integral over z' is an integral over the entire object function (recall that the object function becomes zero where there is no inhomogeneity). We assume that the detection does not occur anywhere in the object so that in the above equation z will be either greater than z'(detection in transmission) or less than z' (reflection detection).

Thus for $z >$ object (detection in transmission) we can write

$$\begin{aligned} T_s(\omega_x, \omega_y; z) &= \frac{\mathrm{e}^{-\gamma_\omega z}}{2\gamma_\omega} \int_{-\infty}^{\infty}\int_{-\infty}^{\infty}\int_{-\infty}^{\infty} o(x', y', z') T_0(x', y', z')\, \mathrm{e}^{-\mathrm{i}x'\omega_x}\, \mathrm{e}^{-\mathrm{i}y'\omega_y}\, \mathrm{e}^{+\gamma_\omega z'}\, \mathrm{d}x'\, \mathrm{d}y'\, \mathrm{d}z' \\ &= \frac{\mathrm{e}^{-\gamma_\omega z}}{2\gamma_\omega} \int_{-\infty}^{\infty}\int_{-\infty}^{\infty}\int_{-\infty}^{\infty} o(x', y', z') T_0(x', y', z') \\ &\quad \times \mathrm{e}^{+\gamma_{\omega r} z'}\, \mathrm{e}^{-\mathrm{i}x'\omega_x}\, \mathrm{e}^{-\mathrm{i}y'\omega_y}\, \mathrm{e}^{+\mathrm{i}\gamma_{\omega i} z'}\, \mathrm{d}x'\, \mathrm{d}y'\, \mathrm{d}z' \\ &= \frac{\mathrm{e}^{-\gamma_\omega z}}{2\gamma_\omega} F_{3\mathrm{D}}\{o(\vec{r}) T_0(\vec{r})\, \mathrm{e}^{+\gamma_{\omega r} z}\}|_{\omega_z = -\gamma_{\omega i}} \qquad z > \text{object}. \end{aligned} \tag{32}$$

Similarly for $z <$ object (reflection detection), we can write

$$T_s(\omega_x, \omega_y; z) = \frac{\mathrm{e}^{+\gamma_\omega z}}{2\gamma_\omega} F_{3D}\{o(\vec{r}) T_0(\vec{r})\, \mathrm{e}^{-\gamma_{\omega r} z}\}|_{\omega_z = +\gamma_{\omega i}} \qquad z < \text{object}. \tag{33}$$

In the above equations, $F_{3\mathrm{D}}$ represents the three-dimensional Fourier transform, where now we have transformed with respect to x, y and z. The above says that the two-dimensional (2D) Fourier transform of the scattered thermal wave detected in a plane is proportional to the 3D Fourier transform of the heterogeneity function multiplied by an exponential term and evaluated at $\omega_z = -\gamma_{\omega i}$, the imaginary part of $\gamma_{\omega i}$. This proportionality term is the now-familiar Weyl expansion, depending on γ_ω, which in turn depends on the relative sizes of the spatial frequencies and the thermal wave number. This is the statement of the Fourier diffraction theorem for thermal waves.

Following the development for the standard diffraction theorem, we now further specialize to the case of plane wave illumination. For the case of plane wave illumination, this implies

$$T_0(\vec{r}) = \mathrm{e}^{\pm \mathrm{i}k_0 z} = \mathrm{e}^{\pm \mathrm{i}(k_r + \mathrm{i}k_i) z}. \tag{34}$$

Note that the wave number is now complex and we have written it as $k_0 = k_r + \mathrm{i}k_i$ to express this. We define k_0 to be the root of k_0^2 such that the imaginary part of k_0 is positive. Care must be taken with the signs in order to express the physical fact that the wave attenuates with distance, which implies greater care with the assumption of the geometry than in the ultrasound

case. With purely real k_0^2 as for ultrasound, this care in not necessary as the exponent does not have a decay term and the wave amplitude oscillates without attenuation. In this instance, let us assume that the inhomogeneity is located somewhere such that $z > 0$ and that the illumination is from the left so that we can assume $T_0(\vec{r}) = \mathrm{e}^{+\mathrm{i}k_0 z} = \mathrm{e}^{+\mathrm{i}(k_r+\mathrm{i}k_i)z}$.

With this expression for the illumination function, we can now write for $z >$ the object function (detection in transmission):

$$\begin{aligned} T_s(\omega_x, \omega_y; z) &= \frac{\mathrm{e}^{-\gamma_\omega z}}{2\gamma_\omega} \int_{-\infty}^{\infty}\int_{-\infty}^{\infty}\int_{-\infty}^{\infty} o(x', y', z')\, \mathrm{e}^{\mathrm{i}(k_r+\mathrm{i}k_i)z'} \\ &\quad \times \mathrm{e}^{+\gamma_{\omega r} z'}\, \mathrm{e}^{-\mathrm{i}x'\omega_x}\, \mathrm{e}^{-\mathrm{i}y'\omega_y}\, \mathrm{e}^{+\mathrm{i}\gamma_{\omega i} z'}\, \mathrm{d}x'\, \mathrm{d}y'\, \mathrm{d}z' \\ &= \frac{\mathrm{e}^{-\gamma_\omega z}}{2\gamma_\omega} F_{3\mathrm{D}}\{o(\vec{r})\, \mathrm{e}^{(-k_i+\gamma_{\omega r})z}\}|_{\omega_z=-k_r-\gamma_{\omega i}} \qquad z > \text{object}. \end{aligned} \tag{35}$$

Similarly for $z <$ object function (reflection detection), we can write

$$T_s(\omega_x, \omega_y; z) = \frac{\mathrm{e}^{\gamma_\omega z}}{2\gamma_\omega} F_{3\mathrm{D}}\{o(\vec{r})\, \mathrm{e}^{(-k_i-\gamma_{\omega r})z}\}|_{\omega_z=-k_r+\gamma_{\omega i}} \qquad z < \text{object}. \tag{36}$$

This is the statement of the Fourier diffraction theorem for thermal waves and specialized to plane wave illumination.

5. Discussion

Equations (32) and (33) are the most general form of the Fourier diffraction theorem for thermal waves. It can be readily observed that the triple integrals are scaled Fourier integrals evaluated at $(\omega_x, \omega_y, \pm\gamma_{\omega i})$ of the object function multiplied by both the illumination function and an exponential function. The negative sign is taken for measurements in transmission and the positive sign for reflection measurements. The exponential decay is due to the attenuative property of thermal waves. It can also be noted that the only mathematical operations occurring in the integrand are multiplications of functions.

Equations (35) and (36) are the statement of the Fourier diffraction theorem for thermal waves where the illumination function has been specialized to plane wave illumination. Note that the triple integrals are scaled Fourier integrals evaluated at $(\omega_x, \omega_y, k_r \pm \gamma_{\omega i})$ of the object function multiplied by an exponential function. Once again, the negative sign is taken for measurements in transmission and the positive sign for reflection measurements.

A two-dimensional version of the standard Fourier diffraction theorem can be found in (Slaney and Kak 1988). In order to compare their result with the one found here, we rewrite the standard Fourier diffraction theorem in three-dimensions and using the same notation as in the current development. This gives

$$T_s(\omega_x, \omega_y; z) = \frac{\mathrm{e}^{-\mathrm{i}\gamma_{\omega i} z}}{2\gamma_\omega} F_{3\mathrm{D}}\{o(\vec{r})\}|_{\omega_z=-k_r-\gamma_{\omega i}} \qquad z > \text{object} \tag{37}$$

$$T_s(\omega_x, \omega_y; z) = \frac{\mathrm{e}^{\mathrm{i}\gamma_{\omega i} z}}{2\gamma_\omega} F_{3\mathrm{D}}\{o(\vec{r})\}|_{\omega_z=-k_r+\gamma_{\omega i}} \qquad z < \text{object}. \tag{38}$$

We note when comparing the thermal wave version of the Fourier diffraction theorem with the standard Fourier diffraction theorem that the thermal wave version differs primarily by additional exponential terms. There is an additional overall exponential attenuation term outside the integrals that is a function of the location of the plane of detection. The triple integrals are the Fourier transform of the object multiplied by a frequency-dependent attenuating exponential. This is entirely due to the complex nature of the wave vector k. If

k were purely real, as is the case for acoustic or electromagnetic waves, then the attenuating exponentials would become unity because both k_i and $\gamma_{\omega r}$ become zero. Thus the triple integrals become the Fourier transform of the object, the attenuating exponential becomes unity and the thermal Fourier diffraction theorem becomes the standard Fourier diffraction theorem.

It remains to determine which values of the three-dimensional Fourier transform of the object are contained in the Fourier transform of the detected image. Let us define the thermal diffusion length of a material as (Mandelis 2001)

$$\mu = \mu(\omega) = \sqrt{\frac{2\alpha}{\omega}}. \tag{39}$$

We note that both k_0 and γ_ω depend on the thermal diffusion length only. That is to say, they depend on the ratio of thermal diffusivity to frequency and not on each of those values independently. The effect of decreasing thermal diffusivity is seen to be similar to that of increasing frequency, both leading to smaller thermal diffusion lengths.

In all cases, for a given (temporal) frequency ω, a three-dimensional subsurface of the full 3D Fourier transform of the object (multiplied by the appropriate exponential) is obtained. For the sake of brevity, we refer to this product of the true object multiplied by the exponential as the object. To clarify the statement of the Fourier diffraction theorem, the object's full 3D Fourier transform is a function of $(\omega_x, \omega_y, \omega_z)$, with each of those spatial frequency variables being independent of the other. However, what we have detected on the plane of detection is a portion of this 3D transform on a subsurface defined by $\omega_z = (-k_r \pm \gamma_{\omega i})$, depending on whether the measurement was made in transmission or reflection. This implies that data at different angles are needed to reconstruct a unique image of the three-dimensional object. The Nyquist sampling theorem will determine the number of required angles. This also explains the ill-posed nature of the problem as observed by other researchers (Nicolaides and Mandelis 1997, Nicolaides *et al* 1997). By making one set of measurements (in transmission or reflection), only a certain portion of the object's three-dimensional Fourier transform has been determined. This is insufficient to uniquely determine the object and leads to an ill-posed problem if an attempt is made to invert the data based on those measurements alone.

Let us examine the shape of the subsurface defined by $\omega_z = (-k_r \pm \gamma_{\omega i})$ for several values of thermal diffusion length. In the limiting case of $\omega = 0$ (the low frequency regime), we note that region is essentially the $\omega_z = 0$ plane. In theory, this would permit easy multi-look Fourier plane reconstruction because no interpolation step is required to map the region into a rectilinear coordinate system. From (39) we see that $\omega = 0$ also implies infinite thermal diffusion length, or as the frequency gets smaller the thermal diffusion length gets longer and the portion of the 3D Fourier transform that we are detecting approaches a plane. For higher temporal frequencies, the region will be a partly curved region and will require interpolation for exact multi-look Fourier plane reconstruction in a rectilinear coordinate system. Figures 1 and 2 show a representative shape of the Fourier region in question. We note that it is indeed a curved region with a peak at the origin and then flattening out to a plane at areas far away from the origin. The size of the 'hump', that is to say the non-plane region, is dependent on the thermal diffusion length. The smaller the thermal the diffusion length, then the wider and higher is the hump. So for long thermal diffusion lengths (or equivalently, low frequencies) the Fourier region in question approaches a plane. This is illustrated in figures 3 and 4 for measurements made in transmission and reflection respectively, where the Fourier region is shown for $\omega_y = 0$ for clarity. For a given value of the thermal diffusion length, as both ω_x and ω_y approach infinity (that is to say, as we move away from the origin), then $\gamma_{\omega i} \to 0, \omega_z \to -\frac{1}{\mu}$. So as we move away from the origin, the Fourier region approaches

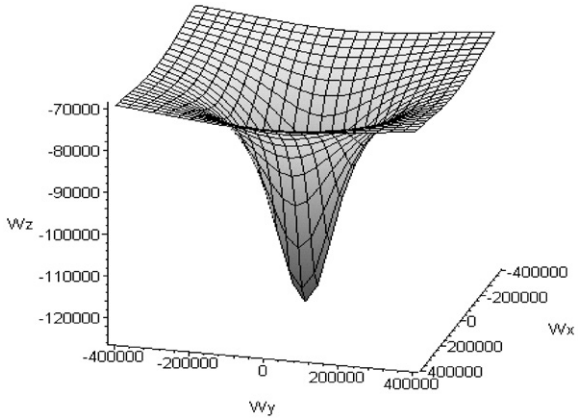

Figure 1. Shape of the 3D Fourier region detected in transmission.

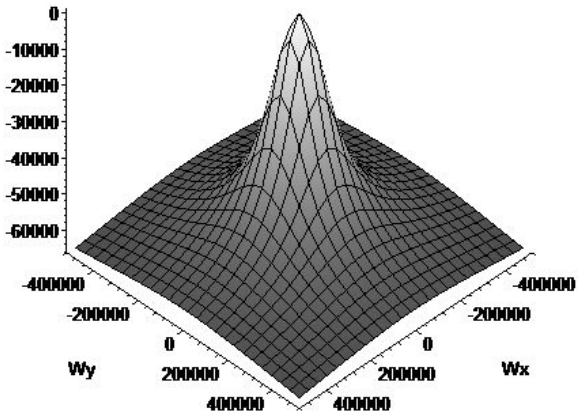

Figure 2. Shape of the 3D Fourier region in reflection.

a ω_z constant plane where that constant is given by the inverse of the thermal diffusion length. We also note that this trend is the opposite as that observed for traditional tomography with ultrasonic waves. In traditional tomography, as the frequency is *increased*, then the Fourier region begins to approach a plane as the sphere in the traditional Fourier region gets flatter and flatter (Slaney and Kak 1988).

6. Applicability of the result

The generation and detection of thermal waves can be done in several ways and is well documented in the literature (Almond and Patel 1996, Mandelis 2001)

A brief overview is given here. An external stimulus is applied to generate a relevant temperature difference which can be detected and used for quantification purposes. A typical experimental set-up might be as seen in figure 5. Several approaches to the generation of thermal waves use periodically modulated laser excitation. However, pulse heating or step heating may also be used. In general, thermal wave studies aim to detect a surface temperature increase due to exponentially attenuated laser excitation and thermal wave scattering due to subsurface inhomogeneities.

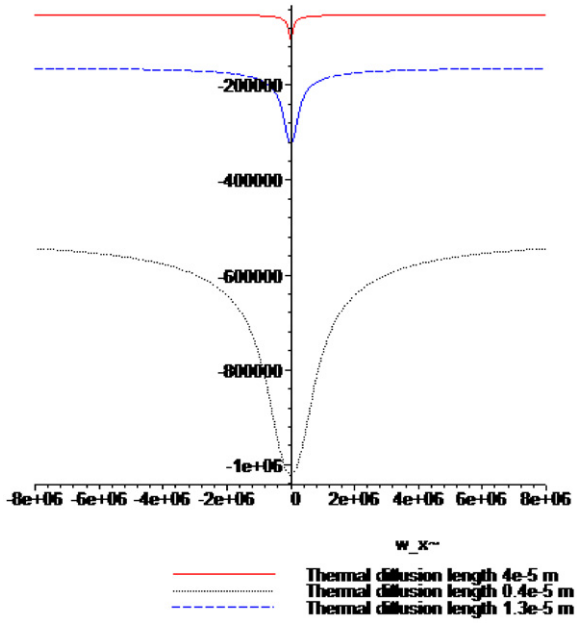

Figure 3. Plot of ω_z (with $\omega_y = 0$) for different thermal diffusion lengths for measurements in transmission.

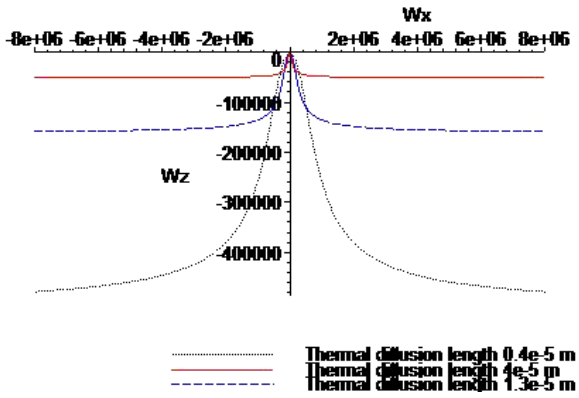

Figure 4. Plot of ω_z (with $\omega_y = 0$) for different thermal diffusion lengths for measurements in reflection.

For pulse heating, the material is subject to a pulse of light with duration ranging from a few milliseconds to a few seconds, depending on the thermal conductivity of the material. The temperature of the material first rises during the pulse and then decays because the energy propagates by thermal diffusion. The presence of a defect or object will reduce the rate of diffusion locally. Point, line or surface detection of the thermal response are possible (Maldague 2002). For step heating, the evolution of temperature is monitored during the application of a long, low power pulse. Periodic (sinusoidal) stimulation can also be used. This latter mode is referred to as lock-in thermography. The lock-in terminology refers to the necessity to monitor the exact time dependence between the output signal and the

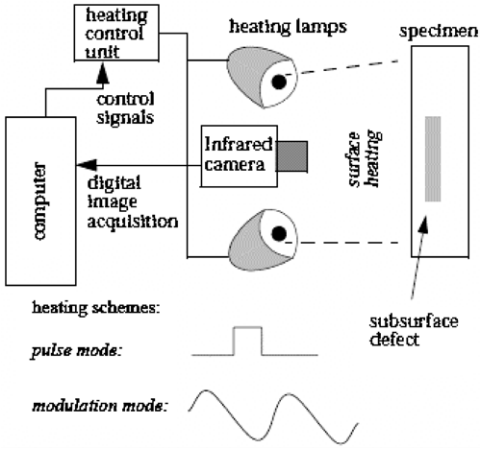

Figure 5. Typical experimental set-up for generation of thermal waves (Maldague 2002).

reference input signal (i.e. the modulated heating). The resulting oscillating temperature field is remotely recorded through its thermal infrared emission. The amplitude and phase of the resulting thermal wave on the specimen can then be observed.

We have shown in previous sections that the Fourier transform of the image on the detection plane is a portion of the full 3D transform of the object. To show that the Fourier diffraction theorem for thermal waves can be used as a basis to develop a reconstruction algorithm, it suffices to show that it is possible to obtain the rest of the full 3D (spatial) transform of the object by suitable choice of experimental configuration. This could be done either by making measurements at different view angles (as is done for x-ray tomography) or by changing the frequency of the illumination—or a combination of both. The change in the illumination frequency can theoretically be achieved with broadband illumination (say pulse heating) and finding the Fourier transform of the time-evolution of the signal. Alternatively, the lock-in approach can be used to make narrow band measurements for a choice of frequencies. Once sufficient 3D Fourier transform data are obtained, the object function can be recovered by spatial 3D inverse Fourier transformation—with the meaning of sufficient being left for investigation under the considerations for the design of an inversion algorithm.

To investigate the achievable coverage of the full 3D Fourier transform, we consider the coverage of the Fourier plane in the first case for varying frequency but fixed view. This could be accomplished with pulse, step or sinusoidal heating. For the sake of clarity, $\omega_y = 0$ is assumed so that only the $\omega_x - \omega_z$ spatial frequency plane is considered, essentially considering a 2D problem instead of 3D. This assumption is made since the analysis would be very similar for the full 3D case but plots in the ω_x–ω_z are clearer. It should be noted that the 2D case would apply if the object and illumination functions were assumed to vary slowly in the y direction and could thus be considered independent of y. In the 2D case, the z detection plane becomes a z detection line. The case for general (unspecified) illumination is shown in figure 6, for which equations (32) or (33) would apply. The case for plane wave illumination is shown in figure 7, for which equations (35) or (36) would apply. In the case of general illumination, the illumination function will need to be known for use after the application of the inverse Fourier transform. From figure 6 (general illumination), we see that as frequency is increased, more and more coverage of the Fourier plane is achieved for both transmission and reflection measurements. Full coverage of the Fourier plane is a sufficient

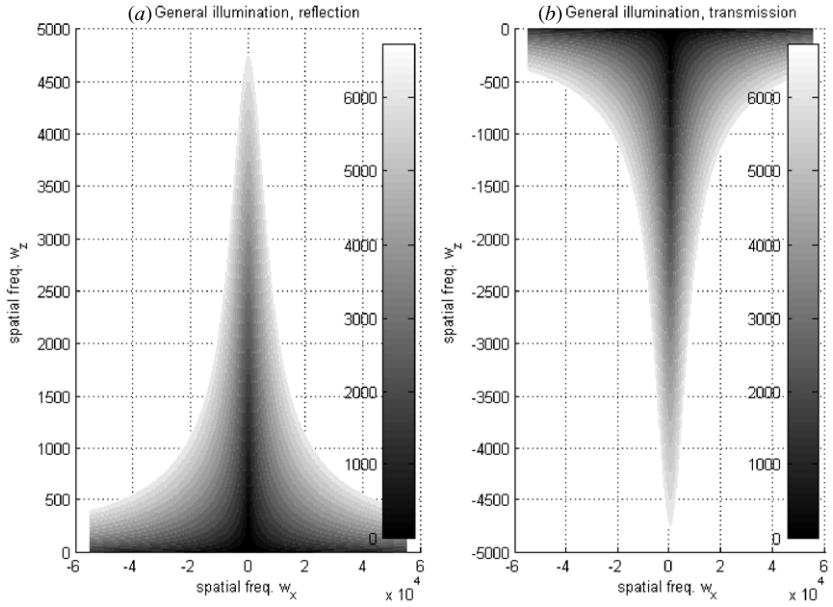

Figure 6. Coverage of Fourier space for constant view and variable frequency. General illumination is assumed.

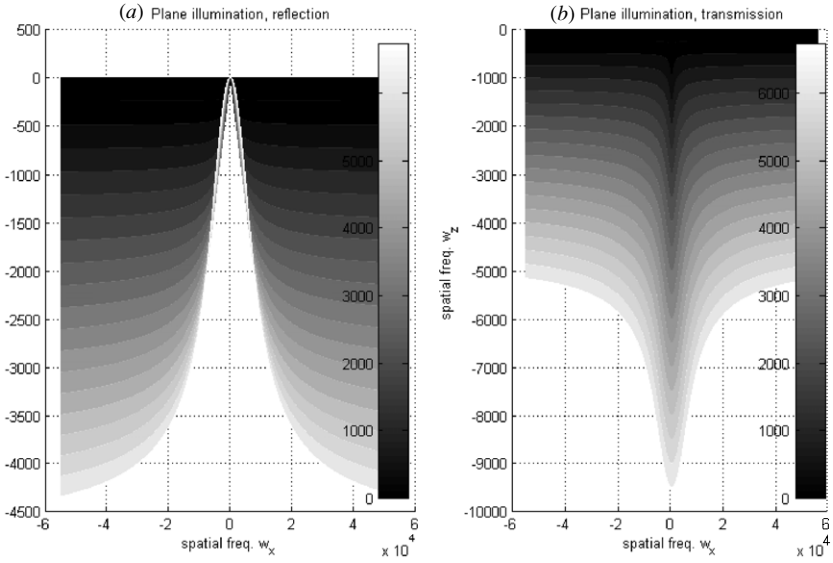

Figure 7. Coverage of Fourier space for constant view and variable frequency. Plane wave illumination.

condition for successful Fourier inversion to occur. The case of plane wave illumination is considered in figure 7. In this case, we see that for measurements made in transmission, complete coverage of the Fourier plane is possible as frequency is increased. However, for measurements made in reflection, complete coverage of the Fourier plane does not occur and

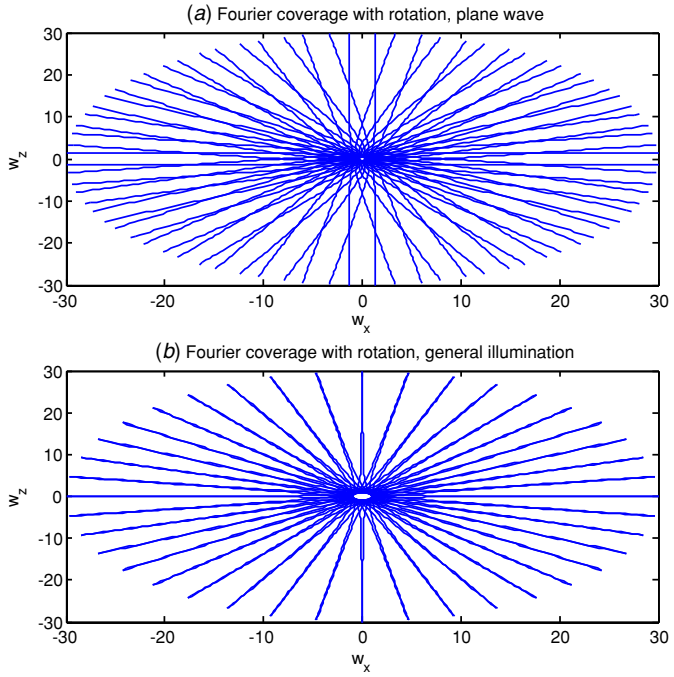

Figure 8. Coverage of Fourier space for constant frequency and multiple view angles. Measurements made in reflection.

low frequency data are missing. This observation leads to the question: how is it possible to obtain less coverage of the Fourier plane with a known (plane) illumination function than with general (unspecified) illumination? The answer to this apparent conundrum is that in the case of a known illumination function, the information contained in this function has been removed from the Fourier (detection) plane. Hence, all the remaining information in the Fourier plane is about the object function. However, for the case of general (unspecified) illumination, the information in the Fourier plane includes information about the illumination function, and this additional information would have to be removed in order to obtain information about only the object function.

As a separate case, we consider the case of making measurements at a fixed (temporal) frequency but at different view angles. This sort of set-up would be similar to those used in x-ray or ultrasound tomography. It must, however, be kept in mind that thermal waves are highly attenuated and do not travel as far as ultrasound. We consider the case of making measurements in reflection or transmission and then obtaining measurements at different view angles, with angles varying from 0 to 2π. The feasibility of this will depend on the sample in question and the given experimental set-up. However, we pursue an idealized situation where data can be obtained from any angle. The reflection results are shown in figure 8 for both general and plane wave illumination. We see that better coverage of the Fourier plane is obtained for the case of plane wave illumination as the general illumination leaves a disc-like gap of data at low frequencies. In comparison, the transmission results are shown in figure 9 for both general and plane wave illumination. For the transmission case, the opposite is true with the general illumination giving better coverage of the Fourier plane than plane wave measurements which leave a low frequency disc of missing data. We note that these results

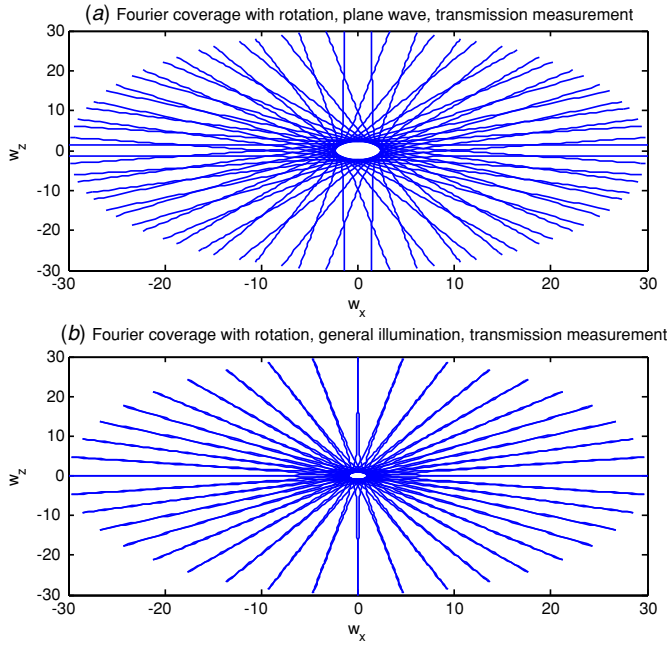

Figure 9. Coverage of Fourier space for constant frequency and multiple view angles. Measurements made in transmission.

are opposite to those that were found for the case of a single view and multiple frequency measurements. For instance, for reflection measurements with plane-waves, poor coverage of the frequency plane was obtained with single view and multiple frequencies but better coverage is obtained with multiple views at a single frequency. It is obvious from this analysis that the choice of illumination function affects the coverage obtained in the Fourier plane, and thus the resolution with which it is possible to perform imaging. Neither transmission nor reflection measurements, plane wave or general illumination, nor single view versus multiple views offer a complete solution to the problem of obtaining data for the entire Fourier plane. However, by suitably choosing the geometry and the illumination function, coverage of the entire Fourier plane *is* possible, so we have shown that thermographic-based tomography is possible. Detailed considerations need to be given to experimental and algorithmic design in order to ensure that enough data have been acquired in order to enable Fourier inversion and thus imaging. Although the intent of this paper was to demonstrate that the Fourier diffraction theorem can be adapted for use for thermal imaging, it has also become obvious the Fourier diffraction theorem can greatly aid in experimental design. By using the Fourier diffraction theorem, we can determine how the choice of geometry and illumination function affect the coverage of the Fourier plane and thus what it should be theoretically possible to 'see' using thermal imaging.

7. Summary and conclusions

In this paper, we have presented the Fourier diffraction theorem for thermal waves. The theorem was presented for the case of a three-dimensional infinite-space domain, in parallel with the traditional development of the standard Fourier diffraction theorem for fields satisfying

the wave equation. The theorem was presented for the cases of both general illumination function and then further specialized to the case of plane wave illumination. It was shown that the values of the 3D Fourier transform of the object (multiplied by an attenuating exponential) that are contained in the Fourier transform of the image on the detection plane are located on the $\omega_z = 0$ plane for low temporal frequencies and on a curved surface for higher temporal frequencies. Because these are subsurfaces of the full 3D Fourier transform, data at different angles and/or different frequencies are necessary to uniquely reconstruct an object. The present work can be used as a basis for developing diffusion-based diffraction tomographic reconstructions algorithms, in a manner similar to the use of the traditional Fourier diffraction theorem. It has also been shown that the choice of detection geometry and the form and frequency of the illumination function greatly affect the obtained coverage of the Fourier domain. The amount of coverage of the spatial Fourier domain is what ultimately determines what it is possible to image. The present work can also be used to aid in experimental design where it can be determined *a priori* how the choice of geometry and illumination function will affect any obtained image.

References

Almond D P and Patel P M 1996 *Photothermal Science and Techniques* (London: Chapman and Hall)

Avdelidis N P, Moropoulou A and Almond D P 2004 Passive and active thermal non-destructive imaging of materials *Proc. SPIE — Int. Soc. Opt. Eng.* **5612** 126–40

Maldague X P V 2002 Introduction to NDT by active infrared thermography *Mater. Eval.* **60** 1060–73

Mandelis A 2001 *Diffusion-Wave Fields, Mathematical Methods and Green Functions* (New York: Springer) p 741

Mandelis A 1991 Theory of photothermal wave diffraction tomography via spatial Laplace spectral decomposition *J. Phys. A: Math. Gen.* **24** 2485–505

Nicolaides L and Mandelis A 1997 Image-enhanced thermal-wave slice diffraction tomography with numerically simulated reconstructions *Inverse Problems* **13** 1393–412

Nicolaides L, Munidasa M and Mandelis A 1997 Thermal-wave infrared radiometric slice diffraction tomography with back-scattering and transmission reconstructions: experimental *Inverse Problems* **13** 1413–25

Pade O and Mandelis A 1994 Thermal-wave slice tomography using wave field reconstruction *J. Physique IV* **4** 7

Quek S, Almond D, Nelson L and Barden T 2005 A novel and robust thermal wave signal reconstruction technique for defect detection in lock-in thermography *Meas. Sci. Technol.* **16** 1223–33

Quek S and Almond D P 2005 Defect detection capability of pulsed transient thermography *Insight, Non-Destr. Test. Cond. Monit.* **47** 212–5

Slaney M and Kak A 1988 *Principles of Computerized Tomographic Imaging* (Philadelphia, PA: SIAM) p 327

Telenkov S A, Vargas G, Nelson J S and Milner T E 2002 Coherent thermal wave imaging of subsurface chromophores in biological materials *Phys. Med. Biol.* **47** 657–71